

results. The behavior shown in Fig. 8 can nevertheless be reconciled with this somewhat disturbing fact if we remember that both channels in our model are in S waves, while in the Frazer-Hendry model, the first channel is in a D wave. If we look in Fig. 9 at the single-channel contributions (given by the dashed lines) to $\text{Re}[U_1 - W_1](U_2 - W_2)$, we see that each has the usual cusp-like behavior at its respective threshold. Since both curves represent S -wave behavior, they have largely the same character and magnitude about their thresholds, and the resultant product which enters into the two-channel solution is thus almost constant between s_1 and s_2 . We emphasize that the shape of this curve is purely a threshold phenomenon and is independent of the poles in the scattering amplitudes. The

effect of poles, so to speak, is simply to amplify the surrounding kinematic behavior. Thus, a pole in the scattering amplitude near the s_1 to s_2 region will tend to stress the flat behavior which occurs in the D function.

We see, in fact, that there is a pole near this region for appropriate values of R corresponding to curves in Fig. 8; namely, on sheet II there is a pole which approaches the point s_1 and eventually emerges on sheet I as a bound state. Because of the flat nature of the curve in Fig. 9, this pole can strongly influence the whole region between s_1 and s_2 and eventually give rise to the uppermost curves of Fig. 8. The shape of the lower cusp-like curves of Fig. 8 is due mainly to the numerator of T_{11} given by $R^2(U_2 - W_2)$, whose real part is plotted in Fig. 9.

Polarization of Recoil Protons in $\pi^\pm p$ Elastic Scattering Near 600 MeV*

RICHARD D. EANDI, THOMAS J. DEVLIN,† ROBERT W. KENNEY, PAUL G. MCMANIGAL,‡
AND BURTON J. MOYER

Lawrence Radiation Laboratory, University of California, Berkeley, California

(Received 15 June 1964)

Angular distributions of recoil-proton polarization in elastic $\pi^\pm p$ scattering were measured at 523-, 572-, and 689-MeV incident pion kinetic energy. Polarization measurements were made by observing the azimuthal asymmetry in the subsequent scattering of recoil protons in large carbon-plate spark chambers. Typical strong variation of the polarization with pion scattering angle near the πp diffraction minima was observed. Since existing opinion favors a D_{13} resonance at 600 MeV, a phase-shift analysis was attempted in order to confirm the existence and parity of this resonance. Available πp total and differential cross sections, these polarization data, and some possible restrictive assumptions related to the 600-MeV resonance were used in the analysis. Though the polarization results aided significantly in restricting the number of acceptable phase-shift sets, still, many plausible and qualitatively different sets were found.

I. INTRODUCTION

PRESENT knowledge of the natures of the various maxima occurring in the pion-nucleon cross sections,^{1,2} for pion kinetic energies below 1.6 BeV (lab), includes quite certain assignments of angular momenta. Parities are, however, not confidently understood except in the well-known case of the " P_{33} " resonance (isotopic spin $T = \frac{3}{2}$, angular momentum $J = \frac{3}{2}$), occurring in pion scattering at 200-MeV kinetic energy in the laboratory frame, or 1238-MeV total energy in the πN center-of-mass frame.

Angular distribution in photoproduction³⁻⁵ and in

elastic scattering^{6,7} have allowed assignments of angular momentum to the phenomena here of interest as follows⁸:

Isotopic spin	Pion K. E. (Lab)	πN total c.m. energy	J
3/2	200 MeV	1238 MeV	3/2
1/2	600 MeV	1512 MeV	3/2
1/2	900 MeV	1688 MeV	5/2
3/2	1350 MeV	1920 MeV	7/2.

Our particular concern in this article is the phenomenon at 1512-MeV c.m. energy. Angular distribution measurements⁸ infer that a $J = \frac{3}{2}$ amplitude is strong at this energy; but other amplitudes are not

* This work was supported by the U. S. Atomic Energy Commission.

† Present address: Princeton University, Princeton, New Jersey.

‡ Present address: Aeronutronic Division, Ford Motor Company, Newport Beach, California.

¹ J. C. Brisson, J. F. Detouff, P. Falk-Vairant, L. van Rossum, and G. Valladas, *Nuovo Cimento* **19**, 210 (1961).

² Thomas J. Devlin, Burton J. Moyer, and Victor Perez-Mendez, *Phys. Rev.* **125**, 690 (1962).

³ Ronald F. Peierls, *Phys. Rev.* **118**, 325 (1960).

⁴ F. P. Dixon and R. L. Walker, *Phys. Rev. Letters* **1**, 458 (1958).

⁵ J. I. Vette, *Phys. Rev.* **111**, 622 (1958).

⁶ Burton J. Moyer, *Rev. Mod. Phys.* **33**, 367 (1961).

⁷ Jerome A. Helland, Thomas J. Devlin, Donald E. Hagge, Michael J. Longo, Burton J. Moyer, and Calvin D. Wood, *Phys. Rev. Letters* **10**, 27 (1963).

⁸ Jerome A. Helland, Calvin D. Wood, Thomas J. Devlin, Donald E. Hagge, Michael J. Longo, Burton J. Moyer, and Victor Perez-Mendez, *Phys. Rev.* **134**, B1079 (1964); Jerome A. Helland, Thomas J. Devlin, Donald E. Hagge, Michael J. Longo, Burton J. Moyer and Calvin D. Wood, *ibid.*, **134**, B1062 (1964).

small, so that it is difficult to conclude that the behavior in this region is simply due to a single state in resonance. This observation is expressed also by those performing recent photoproduction measurements through this energy range.⁹

Peierls' early speculative assignment³ of a " $D_{3/2}$ resonance" at this energy is still tentatively retained. In fact it is supported by experimental measurements of proton recoil polarization in photoproduction experiments in the energy regions immediately below^{10,11} and above¹² the 1512-MeV position, as interpreted after the theoretical arguments of Sakurai,¹³ Moravcsik,¹⁴ and Shaw.¹⁵ But recent recognition of the plurality of significantly strong amplitudes in this region^{9,16} makes it desirable to test the uniqueness of the $D_{3/2}$ assignment. In particular, in view of the Minami ambiguity,¹⁷ we here investigate whether or not a $P_{3/2}$ assignment could be compatible with angular distributions and polarization measurements obtained in elastic πN scattering through the region containing the 1512-MeV phenomenon.

II. EXPERIMENTAL METHOD

A measurement of the polarization of the recoil proton in πp scattering requires that one look for an azimuthal asymmetry in a subsequent scattering of the proton by a suitable polarization analyzer. From the conservation of parity in strong interactions it can be shown that the proton polarization is perpendicular to the plane of scattering. The magnitude of the polarization P is determined from the angular distribution of the recoil proton scattered by the analyzer according to the expression¹⁸

$$\sigma(\theta, \phi, T) = \sigma_0(\theta, T) [1 + PA(\theta, T) \cos \phi],$$

where $A(\theta, T)$ is the analyzing power of the second scatterer for collisions in which protons of energy T are deflected through an angle θ , ϕ is the azimuthal angle between planes of the first and second scatter, and σ_0 is the cross section for unpolarized protons.

In this experiment, two carbon-plate spark chambers were used as analyzer detectors. Their high angular resolution and wide angular acceptance, sharp energy

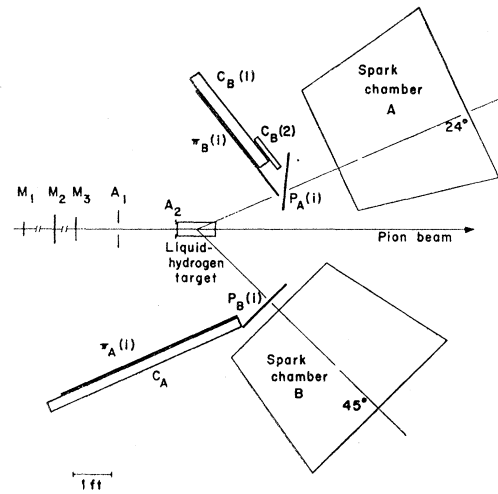


Fig. 1. Plan view of the experiment, showing the orientation of spark chambers and corresponding counters used to select desired events.

resolution, and large sensitive volume allowed the simultaneous measurement of recoil proton polarization over a wide angular range. The spark chambers were triggered by an array of scintillation and Čerenkov counters which identified the particle entering the chambers as recoil protons from elastic pion-proton scattering.

The experimental setup is shown in Fig. 1. The pions were produced by bombarding an aluminum oxide ceramic target with the circulating beam of protons in the bevatron. The pions traversed the apparatus of another experiment⁸ and were refocused by means of a quadrupole on our target. The central momentum, the momentum spread ($\Delta P/P = \pm 3\%$), and the composition of the beam were determined by a magnetic beam-transport system of this upstream experiment. The pion beam was monitored by counters M_1 , M_2 , and M_3 before entering the hydrogen target. A_1 and A_2 were annular anticoincidence counters for further defining the pion beam. Each spark chamber had four identical channels (distributed in azimuthal angle, although only one can be illustrated in Fig. 1) each consisting of a pion counter $\pi(i)$, a proton counter $p(i)$ ($i=1,2,3,4$), and a Čerenkov counter C . Each channel selected elastic scattering events by imposing the condition that the incident pion and the two scattered particles be coplanar. To insure that only protons entered the chambers, the scattered pion was detected by a water Čerenkov counter which would not respond to protons. The kinematically conjugate counter was then assumed to count the recoil proton. Recoil protons scattering from the hydrogen target with their polar angles between 13 and 40 deg were detected by chamber A; angles between 32 and 65 deg by chamber B.

The electronic logic arrays used to trigger the chambers were identical. Either chamber was triggered on the following signature: $M_1 M_2 M_3 C A_1 A_2 p(i) \pi(i)$.

⁹ M. Beneventano, R. Finzi, L. Mezzetti, L. Paoluzi, and S. Tazzari, *Nuovo Cimento* **28**, 1464 (1963).

¹⁰ J. O. Maloy, G. A. Salandin, A. Manfredini, V. Z. Peterson, J. I. Friedman, and H. Kendall, *Phys. Rev.* **122**, 1338 (1961).

¹¹ R. Querzoli, G. Salvini, and A. Silverman, *Nuovo Cimento* **19**, 53 (1961).

¹² C. Mencuccini, R. Querzoli, and G. Salvini, *Phys. Rev.* **126**, 1181 (1962).

¹³ J. J. Sakurai, *Phys. Rev. Letters* **1**, 258 (1958).

¹⁴ Michael J. Moravcsik, *Phys. Rev.* **118**, 1615 (1960).

¹⁵ Peter B. Shaw, *Phys. Rev.* **124**, 1971 (1961).

¹⁶ Detailed elastic scattering measurements at Saclay by a collaboration of Saclay and Berkeley groups have indicated that a $D_{3/2}$ amplitude must be accompanied by a prominent $P_{1/2}$ and $D_{5/2}$ amplitudes (to be published).

¹⁷ Shigeo Minami, *Progr. Theoret. Phys. (Kyoto)* **11**, 213 (1954).

¹⁸ W. S. C. Williams, *An Introduction to Elementary Particles* (Academic Press Inc., New York, 1961), Chap. VIII.

The selection of events other than elastic π - p scattering was minimized by this multiplicity of the coincidence and the stringent coplanarity requirement. The effect of the inelastic background was made insignificant by imposing range requirements on the recoil proton consistent with kinematics for elastic scattering. The ratio of target-full to target-empty counting rate was 20 or greater. The effect of background was all but eliminated by requiring in the film scanning that the particle track, in addition to range requirements, must have its origin in the liquid-hydrogen target when projected back along its direction of flight.

III. DATA ANALYSIS

The calculation of the polarization of recoil protons scattering into a given angular interval was performed in two steps.

First, the spark-chamber film was scanned and each selected scatterer was geometrically and kinematically reconstructed. For each of the two orthogonal views, the proton-carbon scattering angle and sense, the number of carbon plates traversed by the proton before scattering, and the total number of plates traversed before stopping were recorded. From this recorded information the energy T , scattering angle θ , and azimuthal angle ϕ were computed for each selected p -C scatter. Second, the polarization for a given pion scattering angle was then estimated by grouping all the corresponding recoil protons and applying the maximum likelihood method to this event sample. The maximum likelihood theorem¹⁹ states that the value of P is that value which allows the observed array of events in the sample to be consistent with maximum

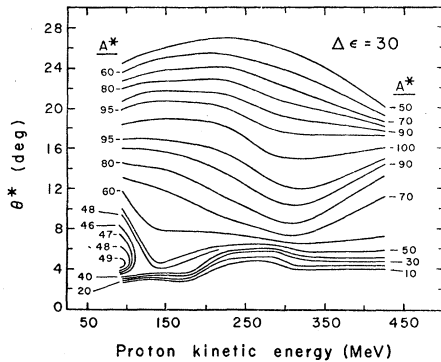


FIG. 2. Curves of constant A^* for p -C scattering, corrected for the inclusion of inelastic scatterings with up to 30-MeV loss ($\Delta\epsilon=30$ MeV). The contours are displayed as a function of laboratory energy of the incident proton T , and angle θ^* . The parameters θ^* and A^* are related to laboratory p -C scattering angle θ_L and real p -C analyzability A by

$$\theta^* = \theta_L (T/180 \text{ MeV})^{1/2} \text{ and } A^* = A/A_{\text{max}}.$$

A_{max} is given in Fig. 3. The use of the starred variables helped suppress predictable, strong variation of the analyzability to simplify use of the plot.

¹⁹ Harald Cramér, *Mathematical Methods of Statistics* (Princeton University Press, Princeton, New Jersey, 1958), p. 498.

TABLE I. Recoil-proton polarization for πN elastic scattering as a function of the cosine of c.m. pion scattering angle. The polarization values quoted were derived by using the effective p -C analyzing power given in Figs. 2 and 3. The errors quoted do not include the error in polarization resulting from uncertainty in analyzing power and systematic errors. (See Sec. III.) Only the statistical uncertainty is shown, the other uncertainties being negligible.

π^+p		π^-p	
523 MeV		523 MeV	
$\cos\theta_{\pi}^*$	Polarization	$\cos\theta_{\pi}^*$	Polarization
+0.250±0.050	-0.26±0.32	+0.250±0.050	-0.94±0.26
+0.150±0.050	-0.34±0.19	+0.150±0.050	-0.94±0.20
+0.050±0.050	-0.42±0.17	+0.050±0.050	-0.34±0.20
-0.050±0.050	-0.44±0.20	-0.050±0.050	-0.02±0.24
-0.175±0.075	+0.20±0.28	-0.150±0.050	-0.78±0.28
-0.325±0.075	-0.56±0.30	-0.275±0.075	+0.38±0.20
-0.475±0.075	-0.10±0.34	-0.400±0.050	+0.42±0.26
-0.625±0.075	-0.36±0.17	-0.525±0.075	+0.10±0.16
-0.775±0.075	-0.14±0.21	-0.675±0.075	+0.10±0.10
		-0.825±0.075	-0.04±0.14

572 MeV		572 MeV	
$\cos\theta_{\pi}^*$	Polarization	$\cos\theta_{\pi}^*$	Polarization
+0.300±0.050	+0.14±0.26	+0.300±0.050	-0.56±0.36
+0.200±0.050	-0.12±0.16	+0.200±0.050	-0.26±0.24
+0.100±0.050	-0.22±0.16	+0.100±0.050	-0.58±0.19
0.000±0.050	-0.30±0.16	-0.025±0.075	-0.36±0.20
-0.100±0.050	-0.12±0.24	-0.175±0.075	-0.18±0.29
-0.225±0.075	+0.38±0.22	-0.300±0.050	+0.64±0.39
-0.375±0.075	+0.64±0.28	-0.400±0.050	+0.12±0.33
-0.525±0.075	+0.44±0.24	-0.500±0.050	-0.10±0.23
-0.650±0.050	+0.22±0.20	-0.600±0.050	-0.62±0.15
-0.775±0.075	-0.14±0.20	-0.700±0.050	-0.58±0.14
		-0.800±0.050	-0.38±0.19

689 MeV		689 MeV	
$\cos\theta_{\pi}^*$	Polarization	$\cos\theta_{\pi}^*$	Polarization
+0.375±0.075	-0.36±0.24	+0.350±0.050	-0.48±0.34
+0.250±0.050	-0.20±0.22	+0.250±0.050	-0.28±0.24
+0.150±0.050	-0.32±0.20	+0.150±0.050	-0.20±0.22
+0.025±0.075	-0.28±0.22	+0.050±0.050	-0.14±0.22
-0.125±0.075	+0.38±0.32	-0.050±0.050	+0.54±0.30
-0.275±0.075	+0.80±0.22	-0.175±0.075	+0.70±0.20
-0.425±0.075	+0.44±0.20	-0.325±0.075	+0.06±0.18
-0.575±0.075	+0.18±0.17	-0.450±0.050	+0.02±0.22
-0.725±0.075	+0.70±0.18	-0.550±0.050	-0.16±0.16
		-0.650±0.050	-0.44±0.16
		-0.750±0.050	-0.24±0.18

probability and thereby maximizes the expression

$$L(P) = \prod_i^{\text{events}} [1 + PA(\theta_i, T_i) \cos\phi_i].$$

The statistical error is arbitrarily defined as that increment of P which makes L/L_{max} equal to $e^{-1/2}$.

The determination of $A(T, \theta)$ was limited by the momentum resolution of the beam transport system, and by the one inch thickness of the carbon plates. This limited our ability to determine the elasticity of a given p -C scatter. In our case the energy resolution, determined by investigating the energy distribution of the accepted events about the kinematically calculated recoil proton energy, was 30 MeV. To compensate for

TABLE II. Coefficients b_n from the expansion $\frac{P(\theta_\pi^*)\sigma(\theta_\pi^*)}{\sin\theta_\pi^*} = \sum_{n=0}^n b_n \cos^n\theta_\pi^*$, obtained by fitting polarization data only.

Incident-pion energy (MeV)	b_0 (mb)	b_1 (mb)	b_2 (mb)	b_3 (mb)	b_4 (mb)	
π^+p	523	-0.143 ± 0.039	-0.802 ± 0.290	-1.570 ± 0.093	-0.909 ± 0.861	...
	572	-0.052 ± 0.027	-0.307 ± 0.189	-0.058 ± 0.656	0.381 ± 0.655	...
	689	0.003 ± 0.027	-0.427 ± 0.117	-0.940 ± 0.555	-1.021 ± 0.748	...
π^-p	523	-0.217 ± 0.062	-1.674 ± 0.347	-3.115 ± 1.388	-1.795 ± 1.537	...
	572	-0.179 ± 0.043	-1.211 ± 0.313	-0.809 ± 1.278	2.397 ± 1.479	...
	689	0.055 ± 0.041	-0.910 ± 0.308	-2.405 ± 1.116	1.989 ± 4.409	3.284 ± 4.967

this effect, we used²⁰ a modified analyzability which was a function of proton energy and angle; this includes the effect of inelastic scatters with energy losses of up to 30 MeV. This modified analyzability is reproduced in the form of a normalized contour map in Figs. 2 and 3. Events having a p -C scattering angle below $\theta(T/180 \text{ MeV})^{1/2} = 4$ deg and above $\theta(T/180 \text{ MeV})^{1/2} = 24$ deg were rejected. This insured that for the proton-energy interval covered, the p -C analyzability does not change sign. The sign of the recoil proton polarization is consistent with the convention that the polarization is positive in the direction $(\mathbf{P}_i \times \mathbf{P}_f)$, where \mathbf{P}_i and \mathbf{P}_f are the initial and final pion momenta, respectively.

The average detection efficiencies were measured separately for left and right scattering by comparison of the same film scanned by different scanners. Also a portion of the film was reversed, such that left-right appeared right-left, and rescanned. The left and right efficiencies determined by this repeated scanning were found to be the same within statistics. No significant asymmetry normal to the πp scattering plane was found for the accepted p -C events. Bias effects are concluded negligible in comparison to the large inherent statistical uncertainty. The uncertainty in the polarization resulting from the uncertainty in the analyzing power can be obtained by investigating the changes in the calculated polarization when the analyzability is modified within the limits of the error in $A(T, \theta)$ obtained from p -C scattering experiments. Thus the parameter $A(T, \theta)$ was altered ± 0.05 , corresponding to the average empirical uncertainty of the p -C scattering experiments, and the polarization recalculated. The deviation from quoted values depended on the make-up of the sample. Average deviation in polarization was 0.03. This test of sensitivity of the data due to a systematically high or low analyzability gives an upper limit of the possible deviation in polarization, since it is highly unlikely that the p -C scattering measurements are either all high or all low.

Table I gives the resulting polarization $P(\cos\theta_\pi^*)$ determined in this experiment for 523-, 572-, and 689-MeV incident pion energy, where θ_π^* is the c.m. pion scattering angle.

²⁰ Vincent Z. Peterson, Lawrence Radiation Laboratory Report UCRL-10622 (unpublished).

IV. DISCUSSION OF RESULTS

It is well known that the product of the polarization and the differential cross section at a given energy can be written as a power series in $\cos\theta_\pi^*$:

$$\frac{P(\theta_\pi^*)\sigma(\theta_\pi^*)}{\sin\theta_\pi^*} = \sum_{n=0}^{2(l_{\max})-1} b_n \cos^n\theta_\pi^*,$$

where the b 's are linear combinations of products between partial-wave amplitudes, and l_{\max} is the state of maximum angular momentum involved in the scattering.¹⁴ A least-squares fit was made of this cosine power series to the polarization data. The series was terminated by applying standard statistical tests. The results are given in Tables II and III. These tables show that

TABLE III. Values of χ^2 and $(\chi^2/D)^{1/2}$, and number of data points used for the order fit chosen.

Incident-pion energy (MeV)	No. of data points	Order of fit, N	Degrees of freedom, D	χ^2	$(\chi^2/D)^{1/2}$	
π^+p	523	9	3	5	6.00	1.10
	572	10	3	6	3.91	0.81
	689	9	3	5	7.41	1.22
π^-p	523	12	3	8	9.79	1.10
	572	11	3	7	4.83	0.83
	689	11	4	6	2.66	0.67

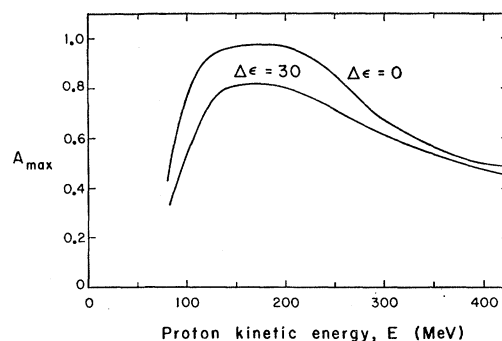


FIG. 3. Curve of A_{\max} as a function of incident-proton kinetic energy. A_{\max} is the largest magnitude the analyzability A ever attains between zero degrees and the first diffraction minimum for incoming protons of a given energy.

TABLE IV. Two plausible sets of phase shifts consistent with all the $\pi^{\pm}p$ total and differential cross sections, real part of forward scattering amplitude, and polarization data. Phase shift set I is consistent with a D_{13} resonant behavior at 600 MeV; set II with a P_{13} resonance. Each set was obtained by starting the respective search with a set of initial phase shifts favoring the desired resonant behavior.

State $l_2 T_2 J$	Set I					
	523 MeV		572 MeV		698 MeV	
	δ (deg)	η	δ (deg)	η	δ (deg)	η
$S_{3,1}$	-22.6	0.82	-22.3	1.00	-16.6	1.00
$P_{3,1}$	-1.9	0.83	-6.7	0.79	-9.1	0.65
$P_{3,3}$	155.2	1.00	159.3	1.00	159.7	0.97
$D_{3,3}$	4.6	0.98	2.8	0.98	-4.0	0.85
$D_{3,5}$	-9.4	0.94	-8.0	0.89	0.8	0.93
$F_{3,5}$	-1.0	1.00	0.6	1.00	2.5	0.95
$F_{3,7}$	0.6	1.00	3.5	0.98	1.8	0.96
$S_{1,1}$	-2.4	0.25	-37.6	0.49	-42.4	0.71
$P_{1,1}$	6.1	0.52	21.6	0.71	16.7	0.54
$P_{1,3}$	0.6	1.00	-3.0	1.00	-14.5	0.60
$D_{1,3}$	43.4	0.84	61.7	0.47	151.9	0.40
$D_{1,5}$	4.8	0.93	1.6	0.91	10.7	0.88
$F_{1,5}$	6.0	1.00	17.3	1.00	13.2	0.93
$F_{1,7}$	0.8	0.99	-0.8	0.97	3.9	0.99

State $l_2 T_2 J$	Set II					
	523 MeV		572 MeV		689 MeV	
	δ (deg)	η	δ (deg)	η	δ (deg)	η
$S_{3,1}$	-21.8	0.81	-22.5	0.97	-16.9	1.00
$P_{3,1}$	-1.0	0.84	-7.0	0.80	-6.5	0.64
$P_{3,3}$	155.2	0.99	158.4	0.98	159.2	0.94
$D_{3,3}$	4.9	0.99	2.5	1.00	-3.6	0.86
$D_{3,5}$	-9.9	0.94	-7.4	0.89	0.1	0.94
$F_{3,5}$	-1.0	1.00	-0.8	1.00	2.9	0.97
$F_{3,7}$	0.4	1.00	3.1	1.00	1.5	0.96
$S_{1,1}$	32.6	0.05	7.5	0.18	-10.4	0.49
$P_{1,1}$	18.7	1.00	37.8	0.42	-2.0	0.28
$P_{1,3}$	40.2	0.65	81.3	0.38	133.8	0.58
$D_{1,3}$	10.4	0.96	7.7	1.00	9.2	0.53
$D_{1,5}$	-6.3	0.96	1.5	0.96	5.4	0.95
$F_{1,5}$	1.5	1.00	2.6	1.00	6.0	1.00
$F_{1,7}$	6.6	1.00	5.9	1.00	7.4	0.91

the statistical accuracy of the data of this experiment is unable to resolve the presence or absence of the higher angular momentum states which manifest themselves in the coefficients of higher powers of $\cos\theta_{\pi}$. The lower order coefficients, b_0 and b_1 , are reliably determined, because they did not deviate in magnitude or sign as we increased the order of fit. However b_3 and b_4 tended to depend significantly on the order of fit. This is reflected in the large errors of these coefficients. Also the inclusion of higher order coefficients permitted least-square fits which were unphysical in that they predicted the polarization in the angular region where no polarization data exist to be significantly greater than one. This symptom is due to the inability of the present data to determine the higher order coefficients.

If we accept the results of Table II, then the failure of particular coefficients to dominate the expansion indicates that a large number of states must contribute. If there is one angular momentum state which really dominates in this energy region, its presence is hidden by its interference with the numerous other states. This is confirmed by angular-distribution and photo-

production experiments.^{4,5,9} Therefore, the assumption that the πN interaction at these energies is dominated by the influence of neighboring single-state resonances as proposed by Moravcsik¹⁴ is unfortunately oversimplified.

In order to circumvent the above problem, a method of analysis is needed which: first, inherently contains the condition that the polarization is bounded by unity, and second, makes use of other independent data to further constrain the polarization in the angular region where no polarization data exist. The conventional method for doing this is phase-shift analysis, for this technique provides a simultaneous least-squares fit of all the available data at a given energy.

Since scattering experiments⁸ indicate that no angular momentum states higher than $l=3$ contribute significantly at energies below 1 BeV, an attempt was made to use total² and differential⁸ cross sections and the forward scattering amplitude,²¹ as well as polarization, in order to obtain a best fit to all the observables simultaneously by expressing these observables in terms of a basic set of partial waves.²² This was accomplished by using a computer to search for sets of amplitudes that agree with all the existing data. Sets of phase shifts were obtained for each of the three energies by feeding random sets of phase shifts as input to the computer, then allowing the computer to converge on a best fit. Many phase-shift sets were found. A large number of these solutions gave sets of phase shifts which differed qualitatively from one another. Based upon the data used, the attainment of a unique phase-shift solution was impossible.

But since existing data^{2,3} favor a resonance having the quantum numbers $J=\frac{3}{2}$, $T=\frac{1}{2}$, and either even or odd parity at 600 MeV, a less ambitious attempt was made to find a set of phase shifts at 523, 572, and 689 MeV that would satisfy the following restrictive

TABLE V. Values of χ^2 found for solutions in Table IV.

	523 MeV	572 MeV	689 MeV
Number of data points fitted, N^a	53	57	58
Number of parameters varied ^b	28	28	28
χ^2 , assuming D_{13} resonance	37	62	27
χ^2 , assuming P_{13} resonance	38	54	27
Best χ^2 value ever attained, assuming no resonance ^c	37	55	27
χ^2 expected ^d	25	29	30

^a Experimental data used, besides polarization, were taken from Refs. 1, 2, 8, and 21.

^b If we include up to $l=3$, we have two spin orientations for each angular momentum state except $l=0$, the real and imaginary parts of the phase shifts for each partial wave, and two possibilities for the value of the isotopic spin of each wave, giving a total of 28 independent parameters.

^c This value is the best value of χ^2 obtained by looking at many phase shift sets obtained by random-search procedure.

^d Here χ_{exp}^2 means the number of degrees of freedom; that is, the number of experimental points fitted minus the number of phase shifts varied.

²¹ J. W. Cronin, Phys. Rev. **118**, 824 (1960).

²² W. S. C. Williams, *An Introduction to Elementary Particles* (Academic Press Inc., New York, 1961), Chap. III.

TABLE VI. Values of the coefficients a_n and b_n from the expansions

$$\sigma(\theta_\pi^*) = \lambda^2 \sum_n a_n \cos^n \theta_\pi^* \quad \text{and} \quad \frac{P(\theta_\pi^*) \sigma(\theta_\pi^*)}{\sin \theta_\pi^*} = \lambda^2 \sum_n b_n \cos^n \theta_\pi^*.$$

Calculated from phase-shift set I						
Coefficients ^a	523 MeV		572 MeV		689 MeV	
	π^+p	π^-p	π^+p	π^-p	π^+p	π^-p
a_0	0.21	0.18	0.18	0.17	0.11	0.14
a_1	0.97	0.67	0.94	0.92	0.54	0.60
a_2	1.33	1.02	1.48	1.78	1.58	2.55
a_3	-0.05	-0.06	-0.24	0.14	-0.16	-0.73
a_4	-0.44	0.33	-1.13	0.13	-1.83	-2.28
a_5	0.15	0.05	0.10	0.23	0.26	1.94
a_6	0.00	0.00	0.30	0.08	0.86	1.75
b_0	-0.06	-0.09	-0.03	-0.06	-0.01	0.04
b_1	-0.30	-0.68	-0.17	-0.81	-0.30	-0.52
b_2	-0.48	-1.16	-0.04	-1.84	-0.38	-1.59
b_3	-0.16	-0.88	0.22	-1.28	-0.05	0.07
b_4	0.07	-0.36	0.03	-1.55	0.31	0.98
b_5	0.00	-0.04	-0.01	-0.62	0.01	0.34

Calculated from phase-shift set II						
Coefficients ^a	523 MeV		572 MeV		689 MeV	
	π^+p	π^-p	π^+p	π^-p	π^+p	π^-p
a_0	0.20	0.19	0.18	0.18	0.10	0.14
a_1	0.97	0.78	0.93	1.06	0.53	0.61
a_2	1.33	1.08	1.43	1.96	1.57	2.51
a_3	-0.04	-0.64	-0.20	-0.38	-0.11	-0.69
a_4	-0.43	0.05	-0.96	-0.35	-1.79	-2.33
a_5	0.14	0.58	0.10	0.57	0.21	1.84
a_6	0.00	0.15	0.18	0.46	0.82	1.87
b_0	-0.06	-0.12	-0.03	-0.09	-0.01	0.03
b_1	-0.30	-0.77	-0.16	-0.69	-0.30	-0.55
b_2	-0.51	-0.92	-0.03	-0.77	-0.35	-1.52
b_3	-0.21	-0.06	0.21	0.76	0.03	0.77
b_4	0.04	0.15	0.04	-0.01	0.21	1.13
b_5	0.00	0.03	0.00	0.00	-0.19	-0.67

^a To compare these coefficients with Table II the coefficients must be multiplied by λ^2 ; $\lambda^2 = 2.21, 1.99,$ and 1.60 mb for $T_\pi = 523, 572,$ and 689 MeV, respectively.

assumptions, where (a) and (b) under 2 are alternative choices.

1. The phase shift sets at the three energies must be consistent among themselves and agree with the lower-energy phase shifts.²³ This demands that the value of the phase shift for each state must vary smoothly with energy, as expected from causality.

2. (a) A D -wave, isospin $\frac{1}{2}$, angular momentum $\frac{3}{2}$, highly absorptive resonance exists at 600 MeV.

(b) A P_{13} rather than a D_{13} resonance exists at 600 MeV. The two states [2(a) and (b)] have the same angular distribution and total cross section since they possess the same J value (Minami ambiguity). Thus with the inclusion of the polarization data of this experiment, we hoped to satisfy either one set of assumptions or the other, and thereby resolve the parity of the resonant state. It must be remembered that phase shifts that satisfy one of the above sets of restrictions would be only a plausible, nonunique solution to the problem. Nevertheless, it would establish that all the available $\pi^\pm p$ data are consistent with either

a P_{13} resonant state as predicted by Wilson,²⁴ or a D_{13} resonant state as predicted by Peierls.³

With this in mind, we introduced sets of phase shifts favoring the D_{13} case to the computer as input information. The computer was then permitted to vary all the phase shifts and obtain solutions at each energy which one hoped would preserve the qualitative behavior of the original input set. The same procedure was followed for the P_{13} case. A consistent and plausible set of phase shifts was found at each energy for both cases; these are given in Table IV. Table V gives the pertinent information concerning the best-fit criteria. Values of the coefficients of the cosine power series for polarization and differential cross sections, calculated from these phase shifts, are tabulated in Table VI. The polarization coefficients for both cases, the P and D resonance possibilities, are essentially the same as the b 's obtained by fitting just the polarization data (Table II). Any differences may be explained by the additional constraints imposed upon the polarization in the angular region where no polarization data exist. The differential-cross-section coefficients are in essential agreement with Helland *et al.*,⁸ whose coefficients were obtained by fitting only angular distribution data.

Qualitatively, the phase-shift sets for both cases have a reasonable behavior with respect to incident-pion

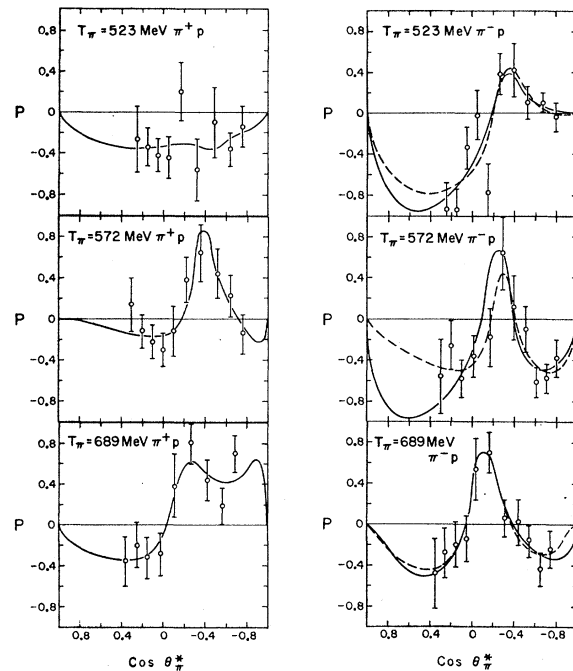


FIG. 4. Differential polarization curves, computed by using the plausible phase shift sets given in Table IV, plotted along with the experimental data. The solid-line curves are those computed from phase-shift set I consistent with a D_{13} resonance at 600 MeV. The dashed-line curves are computed from set II, consistent with a P_{13} resonance. If a dashed-line curve is not shown it means that for all practical purposes the two curves are the same.

²³ Olav T. Vik and Hugo R. Rugge, Phys. Rev. **129**, 2311 (1963).

²⁴ Robert R. Wilson, Phys. Rev. **110**, 1212 (1958).

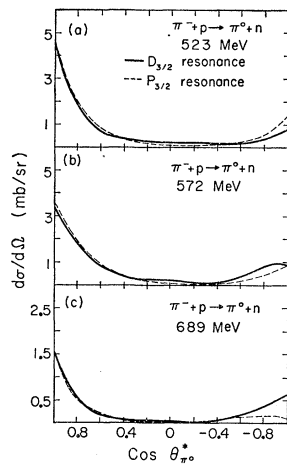


FIG. 5. Charge exchange ($\pi^- + p \rightarrow \pi^0 + n$) differential cross sections computed from the phase-shift sets given in Table IV.

energy. The strong S - and P -wave absorption in the $T = \frac{1}{2}$ channel is consistent with the behavior of the cross section for pion production observed at these and lower energies.²⁵ The only significant departure in their behavior is in the phase shift for the $J = \frac{3}{2}$, $T = \frac{1}{2}$ P - or D -wave state, which possesses an assumed resonant behavior at 600 MeV. That both cases agree with the abundant $\pi^\pm p$ data available is an indication that the accuracy of the polarization data must be improved before the parity of the given state can be determined. Although the D_{13} case is favored by the various πN and $\pi\pi$ isobar models proposed by Peierls²⁶ and Ball and Frazer²⁷ to explain the higher energy maxima, the statistical accuracy of the polarization data measured in this experiment cannot resolve the two cases. This is most strikingly seen in Fig. 4, where the computed curves for both cases are presented.

Figures 5 and 6 show charge exchange polarization and differential cross sections computed from the phase-shift sets given in Table IV. It appears that the charge exchange differential cross section is insensitive to a

²⁵ Janos Kirz, Joseph Schwartz, and Robert D. Tripp, Phys. Rev. **130**, 2481 (1963).

²⁶ Ronald F. Peierls, Phys. Rev. Letters **6**, 641 (1961).

²⁷ James S. Ball and William R. Frazer, Phys. Rev. Letters **7**, 204 (1961).

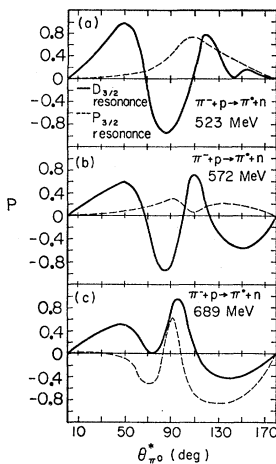


FIG. 6. Differential polarization of the recoil neutron in the interaction $\pi^- + p \rightarrow \pi^0 + n$, computed from the phase-shift sets given in Table IV.

resonance in either the D_{13} or P_{13} partial wave at 600 MeV. On the other hand, the charge exchange recoil neutron polarization appears to be quite sensitive to the parity of the resonance. However, this distinctive behavior of the neutron polarization may be due to the qualitatively different behavior of other background partial waves rather than to whether the resonance is D_{13} or P_{13} . In any case, more experimental information, especially recoil proton polarization with smaller errors and recoil neutron polarization in charge exchange, is clearly needed in order to solve for a unique set of angular momentum amplitudes that would completely determine πN scattering at these energies.

ACKNOWLEDGMENTS

We thank Professor V. Z. Peterson for his valuable discussions on how to make optimum use of existing p -C polarization data in order to determine the polarization of incident protons on carbon. We are grateful to Professor Robert J. Cence for the use of his phase-shift search program and for the many useful discussions on the problems of phase shift analysis. We thank Dr. Jerome A. Helland for providing the pion beam; his complete cooperation in the simultaneous use of the beam is gratefully acknowledged.